Using "Hard" Real-Time Dynamic Clamp to Study Cellular and Network Mechanisms of Synchronization in the Hippocampal Formation

John A. White, Fernando R. Fernandez, Michael N. Economo, and Tilman J. Kispersky

Abstract We report on development and use of dynamic-clamp technology to understand how synchronous neuronal activity is generated in the hippocampus and entorhinal cortex. We find that "hard" real-time dynamic-clamp systems, characterized by very small maximal errors in timing of feedback, are necessary for cases in which fast voltage-gated channels are being mimicked in experiments. Using a hard real-time system to study cellular oscillations in entorhinal cortex, we demonstrate that the stochastic gating of persistent Na^+ channels is necessary for cellular oscillations, and that cellular oscillations lead to dynamic changes in gain for conductance-based synaptic inputs. At the network level, we review experiments demonstrating that oscillating entorhinal stellate cells synchronize best via mutually excitatory interactions. Next, we show that cellular oscillations are volatile in the hypothesized "high-conductance" state, thought to occur in vivo, and suggest alternate means by which coherent activity can be generated in the absence of strong cellular oscillations. We close by discussing future developments that will increase the utility and widespread use of the dynamic-clamp method.

1 Introduction

In the 15 years since its introduction to the neuroscience community (Robinson and Kawai, 1993; Sharp et al., 1993), the dynamic-clamp technique has made steady progress toward adoption as a standard technique in cellular electrophysiology. In neurophysiology, dynamic clamp is used for three main purposes:

1) Introducing "virtual" voltage-gated channels into the neuronal membrane (e.g., Dorval and White, 2005; Bettencourt et al., 2008).

J.A. White (✉)
Department of Bioengineering, Brain Institute, University of Utah, 20 S. 2030 E., Salt Lake City, UT 84112, USA
e-mail: john.white@utah.edu

A. Destexhe, T. Bal (eds.), *Dynamic-Clamp*, Springer Series in Computational Neuroscience 1, DOI 10.1007/978-0-387-89279-5_9,

2) Examining responses of neurons to artificial, conductance-based synaptic inputs (e.g., Dorval and White, 2006; Fernandez and White, 2008).
3) Constructing "hybrid" neuronal networks containing both biological and simulated virtual components (e.g., Netoff et al., 2005a, b; see also Canavier et al., this volume).

Our group's interest in the technique dates back a decade. We were collecting voltage-clamp data from stellate cells in entorhinal cortex and using those data to build and study computational models (White et al., 1998a). We argued that "channel noise" (White et al., 2000a; Kispersky and White, 2008), generated by stochastic flicker of voltage-gated persistent Na^+ channels between open and closed states, was necessary to generate robust subthreshold oscillations (White et al., 1998a).

The problem with our argument in 1998 was that we lacked the ability to perform the crucial, well-controlled experiment to prove our point: a direct comparison of current-clamp data with *noisy* and *noiseless* representations of persistent Na^+ channels. We recognized that the dynamic-clamp technique was the best way forward to perform these experiments. We built such a system around real-time extensions of the Linux operating system (Dorval et al., 2001) and used it to confirm our hypothesis (Dorval and White, 2005). The modern version of our system, developed in collaboration with David Christini of Weill Medical College of Cornell (Christini et al., 1999) and Robert Butera of Georgia Tech (Butera et al., 2001), is open-source and freely available for download (http://rtxi.org/).

In this chapter, we review some of the problems we have studied using the dynamic-clamp technique, encompassing all three uses of dynamic clamp mentioned at the beginning of this section. We first describe studies of how precisely timed dynamic-clamp manipulations must be before performance is compromised (Bettencourt et al., 2008). In *Probing Single-Cell Oscillations*, we review studies of how the properties of virtual Na^+ channels affect cellular membrane-potential oscillations (Dorval and White, 2005) and present new data demonstrating that "synaptic gain" (the PSP peak amplitude as a function of the amplitude of the underlying artificial synaptic conductance) changes dynamically during subthreshold voltage oscillations. In *Networks of Coupled Oscillators*, we discuss studies of synchronization in hybrid networks of periodically firing neurons (Netoff et al., 2005a, b). In *Evidence Against the "Cellular Oscillator" Hypothesis*, we present evidence that entorhinal stellate cells do not generate cellular oscillations under in vivo-like conditions (Fernandez and White, 2008). In *Network Oscillations Arising from Rate-Limiting Synaptic Inputs*, we describe how known coherent activity could arise and be stabilized by synaptic interactions rather than cellular oscillations. Finally, in the *Discussion and Conclusions*, we speculate on the future of the dynamic-clamp technique, in particular considering obstacles to be overcome to increase the general use of this powerful approach in neurophysiology.

2 "Hard" Versus "Soft" Real-Time Performance

In dynamic clamping, current is injected through a recording pipette to simulate the actions of voltage- or ligand-gated channels. Because the current through a membrane channel depends instantaneously on transmembrane potential, dynamic-clamp calculations must be performed in real time. The situation is only more complex if one is modeling channels for which the probability of opening or the open-channel conductance depends on membrane potential. In this case, one must determine the conductance and the transmembrane current in real time.

Our current dynamic-clamp system is built around RTAI (https://www.rtai.org/), a patch to the Linux kernel that allows one to construct processes that run in "hard" real time, without unexpected delays or interruptions. Relative to systems that require specialized hardware from commercial vendors (Robinson and Kawai, 1993; Kullmann et al., 2004), our solution gives excellent performance at substantially lower cost. The trade-off is that RTAI can be more difficult to install and use, because most end-users are less familiar with Linux than with commercial operating systems, and because hardware drivers for Linux are not always available and fully debugged. Faced with this problem, some developers have built their systems in the Windows operating system (e.g., Pinto et al., 2001; Hughes et al., 2008), sacrificing hard real-time performance for gains in ease of use for the community at large. Such "soft" real-time systems perform well on average, but do not guarantee real-time performance on every time step, because it is not possible in these systems to disable all interrupt requests from the operating system.

In a recent study (Bettencourt et al., 2008), we sought to understand just how problematic deviations from hard real-time performance are. To this end, we ran computational simulations of a dynamic-clamp system interacting with a neuron. These simulations allowed us to explore how errors in dynamic-clamp performance would be expected to affect recorded data. We also designed a dynamic-clamp protocol to allow us to degrade hard real-time performance in a controlled fashion in electrophysiological experiments. We studied the effects of the numerical solver, time step, and latency (the delay between the beginning of the time step and the moment that the injected current is updated; latency must be less than the time step to allow real-time performance). The numerical solver is crucial: in simulations with virtualized Na^+ channels, the forward Euler algorithm generated errors that were an order of magnitude larger than those seen with fourth-order Runge–Kutta or stiff algorithms for a given time step. In simulated dynamic-clamp experiments, we found that time steps or latencies above 100 μs disrupted spike shape, but did not affect average firing rate. The effect of time step was particularly deleterious for simulations of virtualized Na^+ channels. For simulations of randomly varying time step and/or latency, degradations in performance were bounded by the worst-case scenario (i.e., the largest errors corresponded to the largest observed values of time step and latency, and matched the errors seen with the same fixed values of time step and latency). This result is a bit surprising, because in our simulated experiments, average time step

was accounted for by the simulated dynamic-clamp algorithm, but jitter in timing was not. Our results imply that one can simply study worst-case delays and latencies to characterize the worst-case performance of the system. Of course, average and median performance depend on the entire distributions of latency and time step, not simply the worst-case values.

Interestingly, real-world experiments were substantially more sensitive to errors than simulations. In experiments, we measured evoked action potentials under control conditions (Fig. 1A), then blocked Na^+ channels with tetrodoxin (TTX) and replaced them under dynamic clamp (Fig. 1B, C, D). Even at our fastest time steps under dynamic clamp (Fig. 1B, $dt = 12.5$ μs, minimum possible latency for this calculation), the rising phase of the action potential was abnormally fast and oscillatory instability was evident near the peak of the spike. Several factors likely contribute to the differences between Fig. 1A, B, including inaccuracies of our modeled Na^+ channels and unaccounted for delays imposed by filtering in data acquisition. Inaccuracies grow dramatically with delays: a time step of 25 μs, with a latency 10 μs beyond the minimum possible value, leads to significant "ringing" of the action potential near the peak (Fig. 1C; for experiments, we do not know the exact value of latency, the part of the time step used to perform calculations, but we know in this case that latency is greater than 10 μs and less than 25 μs). With a time step of 100 μs and minimal latency, the action potential is drastically distorted (Fig. 1D). Overall, we found that delays in hard real-time processing of 10–100 μs led to substantial inaccuracies if they occurred during rapid events like Na^+-based action

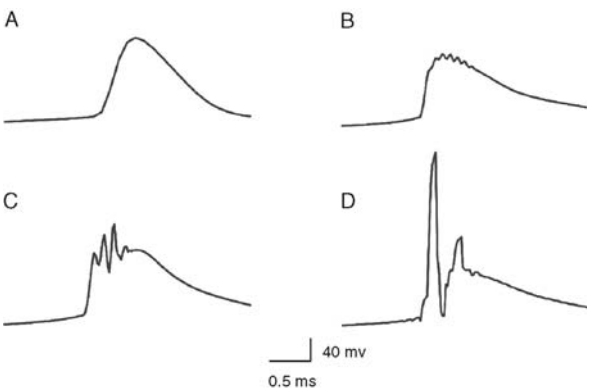

Fig. 1 Dynamic-clamp performance degrades with increased time step and latency. Under whole-cell patch clamp, we recorded depolarization-induced action potentials from a CA1 pyramidal cell. **A**: The action potential under control conditions. **B**: After blocking Na^+ channels with TTX, we replaced them using dynamic clamp. In this case, the time step was 12.5 μs. We solved the Na^+ channel gating equations and output current to the cell as quickly as possible. This implies that latency (the portion of the time step that elapses before current is updated) was the minimum possible value. **C**: The action potential with a time step of 25 μs and the latency increased to 10 μs above its minimal value. **D**: With a time step of 100 μs and minimal latency, the action potential is severely distorted. Adapted from Bettencourt et al. (2008)

potentials. However, for our simulations and experiments, the distortions were short lived: once real-time processing was regained, the system returned quickly to a more accurate solution (Bettencourt et al., 2008).

Is hard real-time performance necessary for effective dynamic clamping? The answer to this question depends on a number of factors:

- For a given soft real-time system and task, how often do uncontrolled interrupts lasting 10–100 μs occur? The answer to this question is likely to depend on the additional demands being placed on the computer and the dynamic-clamp task being performed. We encourage developers and users of soft real-time systems to explore this issue for their applications, as has been done in a recent case (Milescu et al., 2008).
- What sort of membrane mechanism is being simulated? If the timescale of the mechanism is slow compared with the longest uncontrolled interrupts, then hard real time is likely not necessary. Dynamic-clamp-based simulations of voltage-gated Na^+ channels (Fig. 1B, C, D) lie at the other extreme: even miniscule disruptions of hard real-time performance will likely lead to great distortion of results.
- For the hypothesis being tested, how critical is it that the data contain no distorted time steps, and can associated erroneous results be detected and removed before analyzing the data? For example, distortions in spike shape like those seen in Fig. 1C, D would not be difficult to detect in post hoc data analysis. Given our finding that disruptions due to long time steps or latencies are temporary, it should be possible to exclude short time windows around distorted results if they are indeed detectable.

3 Probing Single-Cell Oscillations

We have used dynamic-clamp techniques to study oscillatory behavior in single neurons and neuronal networks. Much of this work has focused on spiny stellate cells of the medial entorhinal cortex, which provide the great majority of the cortical input to the hippocampus (Gloor, 1997). In brain slice recordings, stellate cells generate intrinsic 3–8 Hz subthreshold oscillations in membrane potential (Alonso and Llinas, 1989; Alonso and Klink, 1993). Blocking Na^+ and HCN channels usually (Klink and Alonso, 1993; Dickson et al., 2000) eliminates these oscillations, suggesting that these two populations of channels are most important for generating the phenomenon. Some data (Haas et al., 2007) suggest that other channel populations may be involved as well.

In modeling work (White et al., 1995, 1998a, 2000a), we studied the emergence of subthreshold oscillations and found that the phenomenon was extremely sensitive to model parameters: deviations from ideal parameter values by a 1–5% disrupted the oscillations. Interestingly, accounting for "channel noise" (electrical noise generated by the stochastic opening and closing of membrane-bound ion channels) generated by voltage-gated, non-inactivating Na^+ channels

made modeled membrane-potential oscillations substantially more robust, in that they were supported over a much larger range of parameter space. A similar result was seen in a later study using a more complex model (Fransen et al., 2004).

To test the hypothesis that channel noise enhances 3–8 Hz subthreshold oscillations, we used dynamic clamp to compare control responses (Fig. 2A, B, black traces) with data collected under two experimental conditions: (1) with persistent Na^+ channels blocked (using the drug riluzole) and replaced by a dynamic-clamp representation including channel noise (Fig. 2A, B, dark gray traces) and (2) with persistent Na^+ channels blocked and replaced by a noiseless dynamic-clamp representation (Fig. 2A, B, light gray traces). In this example, stochastic dynamic-clamp results resemble the control case much more closely than noiseless dynamic-clamp results (Fig. 2A, B). Over a population of

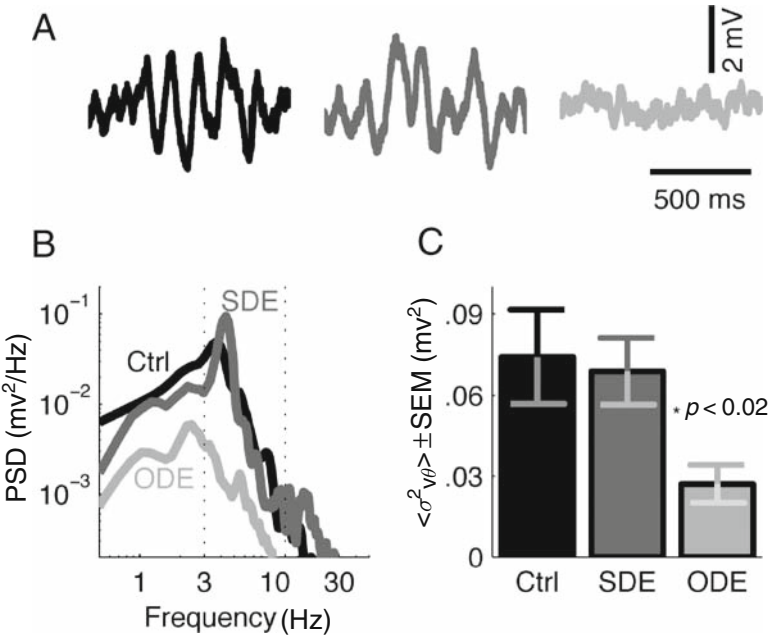

Fig. 2 Channel noise from persistent, voltage-gated Na^+ channels is essential for subthreshold oscillations in entorhinal stellate cells. A: Example subthreshold oscillations, recorded under whole-cell patch clamp from a stellate cell under three conditions. *Black*: control conditions. *Dark gray*: 6 μM riluzole (to block persistent Na^+ channels) plus a dynamic-clamp representation of stochastic differential equation representing the noisy persistent Na^+ channels. *Light gray*: 6 μM riluzole plus a dynamic-clamp representation of ordinary differential equation representing the noiseless persistent Na^+ channels. **B**: Power spectra of long data sets from one stellate cell under the same three conditions. Same color code as in panel A. **C**: Power (mean ± SEM, $n = 14$) in the theta (4–12 Hz) range of frequencies, measured across a population of 14 neurons in each of the three conditions. Same color code as in panel A. Control and stochastic differential equation (SDE) cases are statistically indistinguishable; the ordinary differential equation (ODE) case has substantially less power in the theta (4–12 Hz) band (pair-wise *t*-test, $n = 14$, $p < 0.02$). Adapted from Dorval and White (2005)

recordings, this result holds (Fig. 2C). We also demonstrated that channel noise is necessary to reproduce natural phase-locked responses of stellate cells to weak, 5–8 Hz inputs (Dorval and White, 2005). These results show directly that noise from persistent Na^+ channels has substantial effects on the integrative properties of entorhinal stellate cells. This kind of direct evidence could not be obtained without the benefit of a dynamic-clamp system.

In preliminary data, we have recently shown that subthreshold oscillations can alter the moment-by-moment "gain" describing excitatory postsynaptic potential (EPSP) magnitude for a given conductance input. In these experiments, we depolarized stellate cells to induce subthreshold oscillations, then used dynamic clamp to deliver artificial synaptic input at random times (and thus random phases with respect to the subthreshold oscillations). PSP amplitude clearly varies with the level of depolarization at that moment (Fig. 3A). This effect, which we call

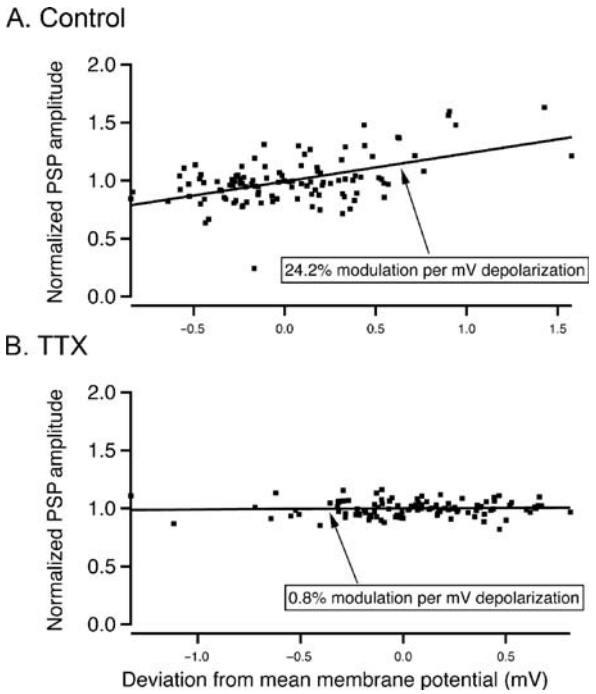

Fig. 3 Entorhinal stellate cells exhibit dynamic gain modulation over the voltage range of subthreshold oscillations. Under whole-cell patch clamp, we depolarized the stellate cell to generate subthreshold oscillations, then used dynamic clamp to deliver artificial "shunting" $GABA_A$-mediated inputs (reversal potential = –60 mV, corrected for junction potential) at random times to measure the effects of membrane potential on IPSP amplitude. **A**: Normalized IPSP amplitude (corrected for driving force) versus the deviation from resting potential, collected under control pharmacological conditions. Small deviations in membrane potential lead to large changes in IPSP amplitude, even with the effects of synaptic driving force accounted for. **B**: With voltage-gated Na^+ blocked using TTX, membrane potential has no effect on drive-corrected IPSP amplitude

dynamic gain modulation, is absent in the presence of the Na^+ channel blocker tetrodotoxin (Fig. 3B). Dynamic gain modulation is present for both inhibitory postsynaptic potentials (IPSPs) and EPSPs and appears independent of effects of synaptic driving force. We hypothesize that this result arises via effects of persistent Na^+ channels on the effective cellular input impedance: at more depolarized potentials, more persistent Na^+ channels are open, giving the appearance of a more resistive membrane because responses to depolarization or hyperpolarizing conductance inputs are larger.

4 Networks of Coupled Oscillators

Subthreshold membrane-potential oscillations in stellate cells have long been speculated to contribute to the theta rhythm, a 4–12 Hz EEG pattern that is believed to be generated by quasi-periodic, synchronized action potentials in the entorhinal cortex and hippocampus (Bland and Colom, 1993; O'Keefe, 1993; Buzsáki, 2002). Two implicit assumptions underlie this speculated mechanism: (1) action potential timing is determined by the subthreshold oscillations and (2) interactions between multiple neurons of this type are such that synchronization is stable. We used dynamic clamp to study the ability of stellate cells to synchronize at theta frequencies (Netoff et al., 2005a, b) via monosynaptic mutual excitation or disynaptic mutual inhibition. In these studies, we took advantage of *phase response analysis* (e.g., Ermentrout and Kopell, 1991; Hansel et al., 1995; Canavier et al., 1997), in which the effects of synaptic inputs to oscillating neurons is reduced to a simple effect on the timing of the next action potential. The main assumptions underlying phase response analysis are that the postsynaptic cell can be considered an oscillator, and that coupling is weak, allowing the effects of a given synaptic input or train of synaptic inputs to be determined via convolution (Ermentrout and Kopell, 1991). In the case that coupling is strong, the basic technique still applies (Acker et al., 2003), although the effect of changing the synaptic waveform (for example) cannot be determined by convolution.

Figure 4 shows results from dynamic-clamp experiments (Netoff et al., 2005b) in which we coupled two entorhinal stellate cells (labeled "E" for *excitatory*). We used two forms of network: one in which we assume mutual excitation via AMPAergic synapses (Fig. 4A) and one in which we assume that excitatory stellate cells communicate by driving inhibitory connections (labeled "I") to their neighbors (Fig. 4B). The depicted data are histograms of the time difference Δt between action potentials in the two stellate cells. The plots contain two peaks because we plotted, for each spike in cell 1, the time of the nearest spikes in cell 2 in both the past and the future. For mutual excitation (Fig. 4A), the two cells synchronize nearly exactly and with very little variance in timing from cycle to cycle (as indicated by the narrowness of the histograms). For mutual inhibition (Fig. 4B), the cells fire nearly out of phase, with

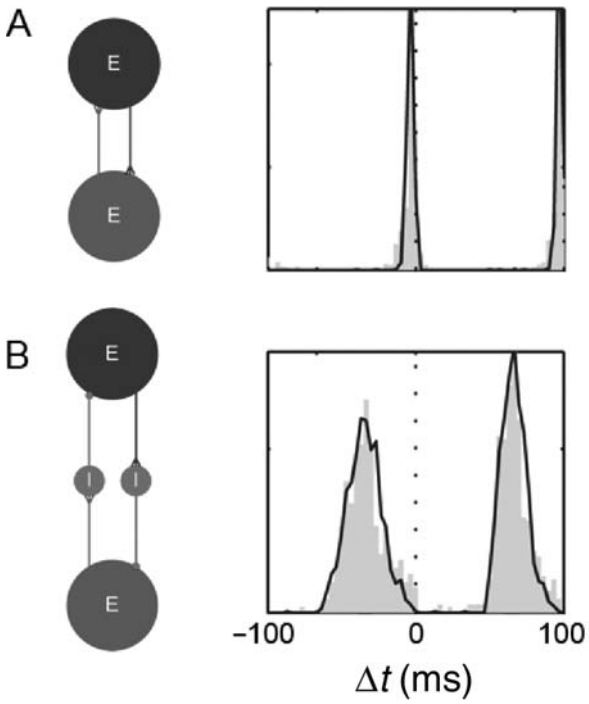

Fig. 4 Entorhinal stellate cells synchronize via mutual excitation but not via mutual inhibition. We recorded from two stellate cells simultaneously and connected them via virtual synapses under dynamic clamp. The diagrams show the two excitatory stellate cells (E) and the structure of the hybrid circuit. The gray bars in the histograms show observed difference in spike times between the two cells. The black lines show predicted time differences from phase response analysis (see text). For both cases, we plotted, for each spike in cell 1, the nearest spike times from cell 2 in both the past and the future. **A**: With virtual AMPAergic synapses between the two cells, they fire nearly synchronously and with small variance in the time difference Δt. Observations match predictions. **B**: With inhibitory interactions between the cells, carried by virtual interneurons giving rise to $GABA_A$-mediated inhibition, the cells do not synchronize and Δt has much larger variance. Again, observations match predictions. Adapted from Netoff et al. (2005b)

substantially more cycle-to-cycle variability. These results were quite consistent across a population of paired recordings (Netoff et al., 2005b).

It should be noted that each panel in Fig. 4 contains two histograms, not one. The gray bars represent observed values of Δt measured when the two stellate cells were connected via virtual synapses. The black lines represent predicted values, calculated based on phase-response measurements taken from each of the cells and combined using established theory. The close correspondence between predicted and observed results demonstrates that the underlying assumptions of phase response analysis hold for these recordings. Thus, we have here an all-too-rare instance in which neurons of immense complexity can

be described accurately as coupled oscillators that simply affect each other's timing. We can understand this system, and scale it to describe very large networks of interconnected neurons (White et al., 1998b), without being required to dissect the biophysical properties that give rise to the behavior.

5 Evidence Against the "Cellular Oscillator" Hypothesis

In the examples of the previous section, the neurons in question were treated as cellular oscillators, with the network frequency determined by the natural firing frequency of the individual cells. This natural firing frequency is in turn often assumed to be determined by the frequency of subthreshold oscillations. For networks involving entorhinal stellate cells, this view of subthreshold oscillations driving spiking behavior and thus network oscillations is prominent in recent modeling work (e.g., O'Keefe and Burgess, 2005; Burgess et al., 2007; Giocomo et al., 2007; Hasselmo et al., 2007). A host of data from recordings in brain slices has been interpreted as supporting this hypothesis (e.g., Alonso and Llinas, 1989; Alonso and Klink, 1993; Dickson et al., 2000; Haas and White, 2002; Fransen et al., 2004; Dorval and White, 2005; Netoff et al., 2005a, b; Haas et al., 2007).

Recent data from our group (Fernandez and White, 2008) call into question the notion that entorhinal stellate cells serve as cellular oscillators in either the subthreshold or suprathreshold regimes. In this work, we used dynamic clamp to flood recorded stellate cells with artificial excitatory and inhibitory synaptic input, effectively putting the neurons in the "high-conductance state" that has been reported from in vivo recordings (Borg-Graham et al., 1998; Destexhe and Pare, 1999; Destexhe et al., 2003). Summary data are shown in Fig. 5. Under control conditions in the brain slice (Fig. 5A), subthreshold oscillations are prominent, with a peak power around 5 Hz. Delivering current-based artificial synaptic input to the cells (Fig. 5B, gray traces) shifts the peak frequency of the subthreshold oscillations, but the cell remains oscillatory. These data are consistent with studies that demonstrate subthreshold resonance in stellate cells and tie this resonance to the intrinsic oscillations (Haas and White, 2002; Erchova et al., 2004; Schreiber et al., 2004; Haas et al., 2007). The situation with *conductance-based* inputs (Fig. 5B, black traces) is much different: responses in this condition are not resonant, containing no peak in the output power spectrum (black power spectral density [PSD] vs. frequency, Fig. 5B). Further study demonstrated that this loss of subthreshold oscillations and resonance was caused by the change in neuronal membrane resistance induced by more realistic conductance-based inputs (Fernandez and White, 2008). A similar effect was seen when we depolarized the stellate cells to induce action potentials in response to artificial synaptic inputs (Fig. 5C). Responses to current-based stimuli showed periodicity in output spike trains (Fig. 5C, gray traces), whereas responses to conductance-based inputs showed no such periodicity (Fig. 5C, black traces). In further dynamic-clamp experiments

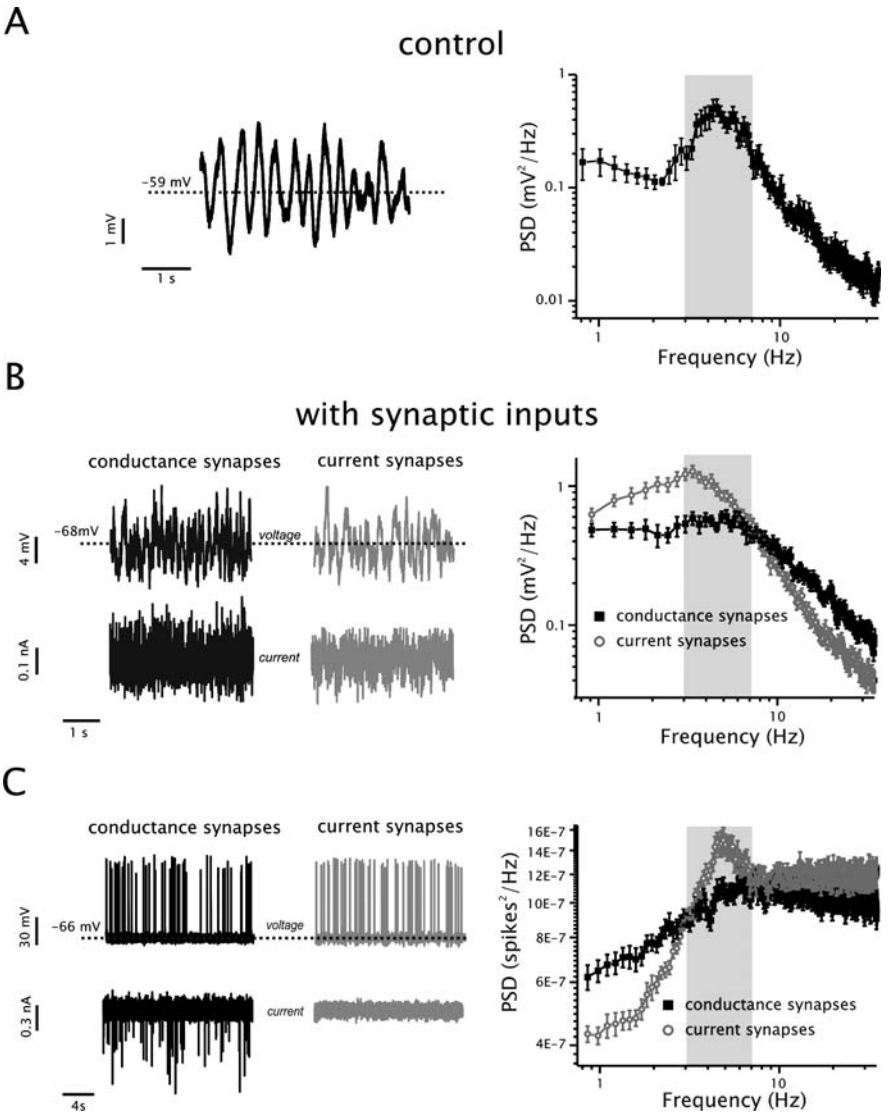

Fig. 5 Conductance-based inputs eliminate subthreshold oscillations, resonance, and intrinsic periodic spiking in entorhinal stellate cells. A: Example raw data (*left*) and power spectral density (PSD, mean ± SEM, $n = 10$) of stellate cell subthreshold voltage responses (average potential ~ –60 mV) under control conditions. **B**: Example responses and average PSD of subthreshold voltage responses under synaptic conductance-based (*black traces*) and current-based (*gray circles*) stimuli ($n = 14$ in each case). Stimuli in both cases were Poisson-process driven trains of artificial $GABA_A$-mediated inhibition and AMPA-mediated excitation. Conductance-based stimuli eliminate the resonance near 3.6 Hz. **C**: With more depolarization, input trains led to spikes. PSDs of spike trains (n = 15 for each case) showed periodic activity with current-based input but not conductance-based input. Adapted from Fernandez and White (2008)

(Fernandez and White, 2008), we demonstrated that conductance-based inputs obliterate periodic spiking in the postsynaptic cell by profoundly altering the shape of spike afterhyperpolarizations.

6 Network Oscillations Arising from Rate-Limiting Synaptic Inputs

The results of Fernandez and White (2008) call into question the widely held hypothesis (see citations above) that cellular oscillations in entorhinal stellate cells are responsible for pacing theta-rhythmic activity in the entorhinal cortex. But if cellular oscillations are not responsible for pacing network oscillations, what other factors might pace the coherent network activity? One attractive hypothesis is that the network is paced by the speed of recovery from chemical synaptic inhibition. Several years ago, we showed in modeling and theoretical work that the typical decay time constant of gamma-amino butyric acid $(GABA)_A$-mediated inhibition is ideal to support stable synchrony for the 40 Hz gamma rhythm (Chow et al., 1998; White et al., 1998b). This finding helped explain previous modeling results (Wang and Buzsáki, 1996). Studies since then have verified the power of mutual inhibition using dynamic clamp to couple neurons artificially, showing that inhibition-based gamma is stable for a wide variety of interneuron classes (Sohal and Huguenard, 2005) and that "shunting" inhibition ($GABA_A$-mediated inhibition with a chloride reversal potential near resting potential) increases the stability of gamma (Vida et al., 2006).

What of the 4–12 Hz theta rhythm? Slow $GABA_A$-mediated inhibition has been described in the hippocampus (Banks et al., 1998), and modeling studies show that slow inhibition could in principle contribute to the local generation of the theta rhythm (White et al., 2000b). More recent studies of theta activity in hippocampal brain slices implicate interactions among pyramidal cells, fast-spiking inhibitory interneurons, and *oriens-lacunosum moleculare* (O-LM) interneurons (Gillies et al., 2002; Gloveli et al., 2005b, a; Rotstein et al., 2005). In such models, two slow variables have been implicated: slow cellular oscillations in O-LM cells (Pike et al., 2000); and slowly decaying $GABA_A$-mediated inhibition from O-LM cells to postsynaptic targets (Maccaferri et al., 2000; Gillies et al., 2002).

We have begun studying the mechanisms by which the theta and gamma rhythms may arise in local hippocampal circuits. Our strategy in this work is to record from one or two neurons and use dynamic clamp to connect these biological neurons with simulated counterparts (Fig. 6A) to construct a "hybrid" network. Given that the high-conductance state disrupts cellular theta oscillations (Fernandez and White, 2008), we have focused on the hypothesis by which slow inhibition from O-LM cells may be the crucial factor pacing neuronal theta rhythms. Our preliminary hybrid network studies show that such a model is plausible. Depending on the level of inhibition from O-LM cells to pyramidal cells and fast-spiking interneurons, this hybrid microcircuit can support either

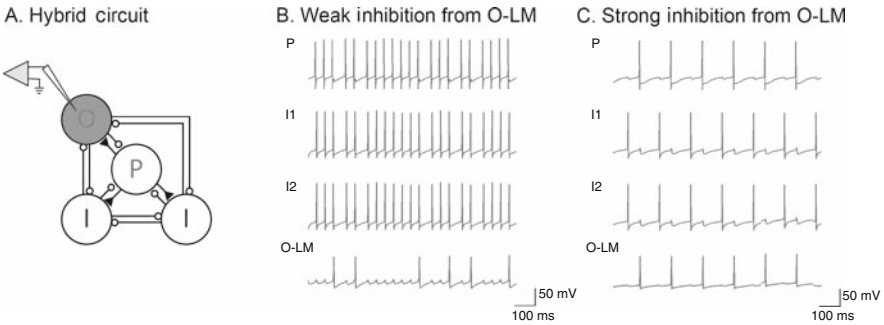

Fig. 6 Gamma and theta rhythms in a hybrid neuronal network. A: Under whole-cell patch-clamp, we recorded from an *oriens-lacunosum moleculare* (O-LM) interneuron and constructed a hybrid network around it based on published data and models (Gloveli et al., 2005b). O: biological O-LM cell. P: virtual pyramidal cell. I: virtual, fast-spiking inhibitory cell. **B**: With relatively weak inhibition from the O-LM cell to the other neurons, the P- and I-cells form a stable gamma rhythm, firing at ~ 40 Hz. The O-LM cell continues to fire slowly in this example. **C**: With strong, slow inhibition from the O-LM cell to the I-cells and P-cell, the network generates a stable theta rhythm

gamma (Fig. 6B) or theta (Fig. 6C) rhythms. The crucial factor in generating slow rhythmic activity in Fig. 6C is that the O-LM cell delivers strong, slow (decay time constant = 20 ms) inhibition to the other cells. In Fig. 6C and similar experiments and simulations, the theta period is roughly proportional to the sum of the decay time constant of O-LM inhibition and that induced by fast-spiking interneurons, which are the first to recover from O-LM inhibition.

7 Discussion and Conclusions

Since its independent introduction to the neurophysiology community by the groups of Marder (Sharp et al., 1993) and Robinson (Robinson and Kawai, 1993), the dynamic-clamp technique has grown steadily in popularity. Still, the technique is only used by a fairly small fraction of the labs that could profit from the technique. We believe that the fruition of the technique will require overcoming a number of barriers:

- The training barrier. Although electrophysiologists have embraced theoretical and mathematical approaches to a greater degree than have most biological and biomedical scientists, the power of the dynamic-clamp technique will likely remain underappreciated until the day when students in neuroscience receive more advanced training in applied mathematics. In particular, familiarity with differential equations and Hodgkin–Huxley style models is crucial for appreciating the power of the dynamic-clamp approach in allowing one to test quantitatively sophisticated hypotheses in living neurons.

- The implementation barrier. Each of the three kinds of dynamic-clamp systems have disadvantages. Linux-based systems still require relatively sophisticated users, particularly at the installation phase. Systems requiring specific real-time hardware are expensive, and do not to our knowledge include specific software for dynamic-clamp applications. Windows systems are the easiest to use and install, but do not include hard real-time performance. Support and documentation for most existing dynamic-clamp systems is not as strong as it should be.
- Barriers in performance. Although dynamic clamp makes entirely new kinds of experiments possible, there are of course limits. Three are worth mentioning here:
  - Modeled voltage- or ligand-gated channels are limited to the site of the recording pipette. This problem could potentially be mitigated by modeling spatially extended neural structures (e.g., dendrites) with the included channels, but doing so is both computationally expensive and difficult to achieve with any confidence of accuracy. For representations of ligand-gated channels, a more direct method would be to uncage the ligand optically, in real time and at the appropriate location(s) (Shoham et al., 2005). Although such uncaging techniques have not, to our knowledge, been tied to a dynamic-clamp system, we believe that this approach is technically feasible.
  - Any model of any membrane mechanism includes inaccuracies. Some, like the assumption of independent activation and inactivation in voltage-gated Na^+ channels, are known to be incorrect (Hille, 2001) but are used anyway. Even with the correct mathematical structure of the model, details of voltage-clamp-based models are wrong due to errors in space clamp and other difficulties. Worse yet, channel densities are often unidentified for a given case, and channel properties are quite sensitive to the neuromodulatory state (Hille, 2001), another unknown. In a recent paper, Milescu et al. (2008) take advantage of a very clever optimization strategy that automatically "tunes" the dynamic-clamp model to match data collected under control conditions. This approach could be extremely important for cases in which the control behavior is known.
  - Finally, dynamic clamp can at present only represent the electrical, not the electrochemical, actions of a given membrane mechanism. As a consequence, dynamic-clamp systems are of limited utility in studying calcium-dependent phenomena like synaptic plasticity. In principle, one could use calcium uncaging to begin to overcome this limitation. In practice, controlling intracellular calcium concentrations in real time is a very daunting challenge, made all the more difficult by the existence of calcium microdomains and fact that calcium indicators invariably distort the "true" calcium waveform. Of the three technical challenges mentioned here, this would seem to be the most daunting.

We do not wish to end on a pessimistic note. Although there is much work to do, we are firmly convinced that the dynamic-clamp approach has a bright

future, destined to assume its place beside current- and voltage-clamp techniques as a "standard" method in cellular electrophysiology.

Acknowledgments We thank past and present students and collaborators on dynamic-clamp work, including M.I. Banks, J.C. Bettencourt, M. Binder, R.J. Butera, D.J. Christini, A.D. Dorval, E. Idoux, K.P. Lillis, N. Kopell, L.E. Moore, T.I. Netoff, P. Randeria , and L. Stupin. This work was supported by grants from the National Institutes of Health (NCRR, NIMH, and NINDS).

References

Acker CD, Kopell N, White JA (2003) Synchronization of strongly coupled excitatory neurons: relating network behavior to biophysics. J Comput Neurosci 15:71–90.

Alonso A, Llinas RR (1989) Subthreshold Na^+-dependent theta-like rhythmicity in stellate cells of entorhinal cortex layer II. Nature 342:175–177.

Alonso A, Klink R (1993) Differential electroresponsiveness of stellate and pyramidal-like cells of medial entorhinal cortex layer II. J Neurophysiol 70:128–143.

Banks MI, Li TB, Pearce RA (1998) The synaptic basis of GABAA,slow. J Neurosci 18:1305–1317.

Bettencourt JC, Lillis KP, Stupin LR, White JA (2008) Effects of imperfect dynamic clamp: Computational and experimental results. J Neurosci Methods 169:282–289.

Bland BH, Colom LV (1993) Extrinsic and intrinsic properties underlying oscillation and synchrony in limbic cortex. Prog Neurobiol 41:157–208.

Borg-Graham LJ, Monier C, Fregnac Y (1998) Visual input evokes transient and strong shunting inhibition in visual cortical neurons. Nature 393:369–373.

Burgess N, Barry C, O'Keefe J (2007) An oscillatory interference model of grid cell firing. Hippocampus 17:801–812.

Butera RJ, Jr., Wilson CG, Delnegro CA, Smith JC (2001) A methodology for achieving high-speed rates for artificial conductance injection in electrically excitable biological cells. IEEE Trans Biomed Eng 48:1460–1470.

Buzsáki G (2002) Theta oscillations in the hippocampus. Neuron 33:325–340.

Canavier CC, Butera RJ, Dror RO, Baxter DA, Clark JW, Byrne JH (1997) Phase response characteristics of model neurons determine which patterns are expressed in a ring circuit model of gait generation. Biol Cybern 77:367–380.

Chow CC, White JA, Ritt J, Kopell N (1998) Frequency control in synchronized networks of inhibitory neurons. J Comput Neurosci 5:407–420.

Christini DJ, Stein KM, Markowitz SM, Lerman BB (1999) Practical real-time computing system for biomedical experiment interface. Ann Biomed Eng 27:180–186.

Destexhe A, Pare D (1999) Impact of network activity on the integrative properties of neocortical pyramidal neurons in vivo. J Neurophysiol 81:1531–1547.

Destexhe A, Rudolph M, Pare D (2003) The high-conductance state of neocortical neurons in vivo. Nat Rev Neurosci 4:739–751.

Dickson CT, Magistretti J, Shalinsky MH, Fransen E, Hasselmo ME, Alonso A (2000) Properties and role of I(h) in the pacing of subthreshold oscillations in entorhinal cortex layer II neurons. J Neurophysiol 83:2562–2579.

Dorval AD, White JA (2005) Channel noise is essential for perithreshold oscillations in entorhinal stellate neurons. J Neurosci 25:10025–10028.

Dorval AD, White JA (2006) Synaptic input statistics tune the variability and reproducibility of neuronal responses. Chaos 16:026105.

Dorval AD, Christini DJ, White JA (2001) Real-time Linux dynamic clamp: a fast and flexible way to construct virtual ion channels in living cells. Ann Biomed Eng 29:897–907.

Erchova I, Kreck G, Heinemann U, Herz AV (2004) Dynamics of rat entorhinal cortex layer II and III cells: characteristics of membrane potential resonance at rest predict oscillation properties near threshold. J Physiol 560:89–110.
Ermentrout B, Kopell N (1991) Multiple pulse interactions and averaging in systems of coupled oscillators. J Math Biol 29:195–217.
Fernandez FR, White JA (2008) Artificial synaptic conductances reduce subthreshold oscillations and periodic firing in stellate cells of the entorhinal cortex. J Neurosci 28:3790–3803.
Fransen E, Alonso AA, Dickson CT, Magistretti J, Hasselmo ME (2004) Ionic mechanisms in the generation of subthreshold oscillations and action potential clustering in entorhinal layer II stellate neurons. Hippocampus 14:368–384.
Gillies MJ, Traub RD, LeBeau FE, Davies CH, Gloveli T, Buhl EH, Whittington MA (2002) A model of atropine-resistant theta oscillations in rat hippocampal area CA1. J Physiol 543:779–793.
Giocomo LM, Zilli EA, Fransen E, Hasselmo ME (2007) Temporal frequency of subthreshold oscillations scales with entorhinal grid cell field spacing. Science 315:1719–1722.
Gloor P (1997) The temporal lobe and limbic system. New York: Oxford University Press.
Gloveli T, Dugladze T, Saha S, Monyer H, Heinemann U, Traub RD, Whittington MA, Buhl EH (2005a) Differential involvement of oriens/pyramidale interneurones in hippocampal network oscillations in vitro. J Physiol 562:131–147.
Gloveli T, Dugladze T, Rotstein HG, Traub RD, Monyer H, Heinemann U, Whittington MA, Kopell NJ (2005b) Orthogonal arrangement of rhythm-generating microcircuits in the hippocampus. Proc Natl Acad Sci USA 102:13295–13300.
Haas JS, White JA (2002) Frequency selectivity of layer II stellate cells in the medial entorhinal cortex. J Neurophysiol 88:2422–2429.
Haas JS, Dorval AD, II, White JA (2007) Contributions of Ih to feature selectivity in layer II stellate cells of the entorhinal cortex. J Comput Neurosci 22:161–171.
Hansel D, Mato G, Meunier C (1995) Synchrony in excitatory neural networks. Neural Comput 7:307–337.
Hasselmo ME, Giocomo LM, Zilli EA (2007) Grid cell firing may arise from interference of theta frequency membrane potential oscillations in single neurons. Hippocampus 17:1252–1271.
Hille B (2001) Ion channels of excitable membranes, 3rd Edition. Sunderland, Mass.: Sinauer.
Hughes SW, Lorincz M, Cope DW, Crunelli V (2008) NeuReal: An interactive simulation system for implementing artificial dendrites and large hybrid networks. J Neurosci Methods 169:290–301.
Kispersky TJ, White JA (2008) Stochastic models of ion channel gating. Scholarpedia 3:1327.
Klink R, Alonso A (1993) Ionic mechanisms for the subthreshold oscillations and differential electroresponsiveness of medial entorhinal cortex layer II neurons. J Neurophysiol 70:144–157.
Kullmann PH, Wheeler DW, Beacom J, Horn JP (2004) Implementation of a fast 16-Bit dynamic clamp using LabVIEW-RT. J Neurophysiol 91:542–554.
Maccaferri G, Roberts JD, Szucs P, Cottingham CA, Somogyi P (2000) Cell surface domain specific postsynaptic currents evoked by identified GABAergic neurones in rat hippocampus in vitro. J Physiol 524 Pt 1:91–116.
Milescu LS, Yamanishi T, Ptak K, Mogri MZ, Smith JC (2008) Real-time kinetic modeling of voltage-gated ion channels using dynamic clamp. Biophys J 95:66–87.
Netoff TI, Acker CD, Bettencourt JC, White JA (2005a) Beyond two-cell networks: experimental measurement of neuronal responses to multiple synaptic inputs. J Comput Neurosci 18:287–295.
Netoff TI, Banks MI, Dorval AD, Acker CD, Haas JS, Kopell N, White JA (2005b) Synchronization in hybrid neuronal networks of the hippocampal formation. J Neurophysiol 93:1197–1208.
O'Keefe J (1993) Hippocampus, theta, and spatial memory. Curr Opin Neurobiol 3:917–924.

O'Keefe J, Burgess N (2005) Dual phase and rate coding in hippocampal place cells: theoretical significance and relationship to entorhinal grid cells. Hippocampus 15:853–866.
Pike FG, Goddard RS, Suckling JM, Ganter P, Kasthuri N, Paulsen O (2000) Distinct frequency preferences of different types of rat hippocampal neurones in response to oscillatory input currents. J Physiol 529 Pt 1:205–213.
Pinto RD, Elson RC, Szucs A, Rabinovich MI, Selverston AI, Abarbanel HD (2001) Extended dynamic clamp: controlling up to four neurons using a single desktop computer and interface. J Neurosci Methods 108:39–48.
Robinson HP, Kawai N (1993) Injection of digitally synthesized synaptic conductance transients to measure the integrative properties of neurons. J Neurosci Meth 49:157–165.
Rotstein HG, Pervouchine DD, Acker CD, Gillies MJ, White JA, Buhl EH, Whittington MA, Kopell N (2005) Slow and fast inhibition and an H-current interact to create a theta rhythm in a model of CA1 interneuron network. J Neurophysiol 94:1509–1518.
Schreiber S, Erchova I, Heinemann U, Herz AV (2004) Subthreshold resonance explains the frequency-dependent integration of periodic as well as random stimuli in the entorhinal cortex. J Neurophysiol 92:408–415.
Sharp AA, O'Neil MB, Abbott LF, Marder E (1993) Dynamic clamp: Computer-generated conductances in real neurons. J Neurophysiol 69:992–995.
Shoham S, O'Connor DH, Sarkisov DV, Wang SS (2005) Rapid neurotransmitter uncaging in spatially defined patterns. Nat Methods 2:837–843.
Sohal VS, Huguenard JR (2005) Inhibitory coupling specifically generates emergent gamma oscillations in diverse cell types. Proc Natl Acad Sci USA 102:18638–18643.
Vida I, Bartos M, Jonas P (2006) Shunting inhibition improves robustness of gamma oscillations in hippocampal interneuron networks by homogenizing firing rates. Neuron 49:107–117.
Wang XJ, Buzsáki G (1996) Gamma oscillation by synaptic inhibition in a hippocampal interneuronal network model. J Neurosci 16:6402–6413.
White JA, Budde T, Kay AR (1995) A bifurcation analysis of neuronal subthreshold oscillations. Biophys J 69:1203–1217.
White JA, Klink R, Alonso A, Kay AR (1998a) Noise from voltage-gated ion channels may influence neuronal dynamics in the entorhinal cortex. J Neurophysiol 80:262–269.
White JA, Chow CC, Ritt J, Soto-Trevino C, Kopell N (1998b) Synchronization and oscillatory dynamics in heterogeneous, mutually inhibited neurons. J Comput Neurosci 5:5–16.
White JA, Rubinstein JT, Kay AR (2000a) Channel noise in neurons. Trends Neurosci 23:131–137.
White JA, Banks MI, Pearce RA, Kopell NJ (2000b) Networks of interneurons with fast and slow gamma-aminobutyric acid type A (GABAA) kinetics provide substrate for mixed gamma-theta rhythm. Proc Natl Acad Sci USA 97:8128–8133.